ESC European Society of Cardiology

Cardiovascular Research (2017) **113**, 1351–1363
doi:10.1093/cvr/cvx089

OxLDL-derived lysophosphatidic acid promotes the progression of aortic valve stenosis through a LPAR1-RhoA–NF-κB pathway

Mohamed Jalloul Nsaibia[1], Marie-Chloé Boulanger[1], Rihab Bouchareb[1], Ghada Mkannez[1], Khai Le Quang[1], Fayez Hadji[1], Deborah Argaud[1], Abdellaziz Dahou[2], Yohan Bossé[2], Marlys L. Koschinsky[3], Philippe Pibarot[2], Benoit J. Arsenault[2], André Marette[2], and Patrick Mathieu[1]*

[1]Laboratory of Cardiovascular Pathobiology, Institut Universitaire de Cardiologie et de Pneumologie de Québec/Quebec Heart and Lung Institute, Research Center, Department of Surgery, Laval University, 2725 Chemin Ste-Foy, Quebec, Quebec G1V-4G5, Canada; [2]Institut Universitaire de Cardiologie et de Pneumologie de Québec/Quebec Heart and Lung Institute, Research Center, Laval University, Quebec, Canada; and [3]Western University, 1151 Richmond St, London N6A-5B7, Ontario, Canada

Received 23 September 2016; revised 28 February 2017; editorial decision 29 April 2017; accepted 3 May 2017; online publish-ahead-of-print 4 May 2017

Time for primary review: 40 days

Aims Oxidatively modified lipoproteins may promote the development/progression of calcific aortic valve stenosis (CAVS). Oxidative transformation of low-density lipoprotein (OxLDL) generates lysophosphatidic acid (LPA), a lipid mediator that accumulates in mineralized aortic valves. LPA activates at least six different G protein-coupled receptors, which may play a role in the pathophysiology of CAVS. We hypothesized that LPA derived from OxLDL may promote a NF-κB signature that drives osteogenesis in the aortic valve.

Methods and results The role of OxLDL-LPA was examined in isolated valve interstitial cells (VICs) and the molecular pathway was validated in human explanted aortic valves and in a mouse model of CAVS. We found that OxLDL-LPA promoted the mineralization and osteogenic transition of VICs through LPAR1 and the activation of a RhoA-NF-κB pathway. Specifically, we identified that RhoA/ROCK activated IκB kinase alpha, which promoted the phosphorylation of p65 on serine 536 (p65 pS536). p65 pS536 was recruited to the *BMP2* promoter and directed an osteogenic program not responsive to the control exerted by the inhibitor of kappa B. In $LDLR^{-/-}$/$ApoB^{100/100}$/IGFII transgenic mice (IGFII), which develop CAVS under a high-fat and high-sucrose diet the administration of Ki16425, a Lpar1 blocker, reduced by three-fold the progression rate of CAVS and also decreased the osteogenic activity as measured with a near-infrared fluorescent probe that recognizes hydroxyapatite of calcium.

Conclusions OxLDL-LPA promotes an osteogenic program in the aortic valve through a LPAR1-RhoA/ROCK–p65 pS536 pathway. LPAR1 may represent a suitable target to prevent the progression of CAVS.

Keywords Calcific aortic valve stenosis • Calcific aortic valve disease • Lysophosphatidic acid • OxLDL • LPAR1 • RhoA • NF-κB • p65 serine 536 • BMP2 • Bone morphogenetic protein 2 • Valve interstitial cells • Mineralization • Calcification • Osteogenic program

1. Introduction

Calcific aortic valve stenosis (CAVS) is a chronic disorder characterized by a progressive mineralization of the aortic valve.[1] Despite the presence of rare osteoclast-like cells in surgically explanted mineralized aortic valves, there is a net balance towards deposition of mineral through an osteogenic process.[2] Though the disease can be diagnosed early in its course by echocardiography there is no medical treatment that can prevent or reduce the progression of CAVS. Chronic low-grade inflammation is an important feature of CAVS.[3] The nuclear factor kappa B (NF-κB) pathway orchestrates the inflammatory response by regulating gene expression pattern, which is cell and context dependent.

* Corresponding author. Institut de Cardiologie et de Pneumologie de Québec/Quebec Heart and Lung Institute, 2725 Chemin Ste-Foy, Québec, Quebec G1V-4G5, Canada. Tel: +1 418 656 4717; fax: +1 418 656 4707, E-mail: patrick.mathieu@fmed.ulaval.ca

Site-specific post-translation modifications of p65, the prototypical NF-κB subunit, define selective gene expression patterns,[4,5] which may play a role during the pathogenesis of CAVS. The activity of NF-κB is controlled by the inhibitor of kappa B (IκBα), which in response to p65 is expressed and is recruited to the nucleus where it complexes with p65 and negatively regulates the expression of genes.[4] The phosphorylation of p65 on serine 536 (p65 pS536) directs the expression of selected genes that are not responsive to the negative regulation exerted by IκBα.[6] Therefore, p65 pS536-target genes escape IκBα-mediated negative feedback control mechanism, which may result in sustained activation of detrimental pathways. Evidence suggests that inflammatory stimuli promote the mineralization of valve interstitial cell (VIC) cultures, but the molecular process whereby inflammation promotes an osteogenic response in the aortic valve is still ill-defined.[3] Whether key osteogenic genes such as *BMP2*, a potent morphogen that induces an osteogenic program by up-regulating *RUNX2*,[7] is under the control of a p65 pS536 signature in VICs is unknown.

Oxidized lipid derivatives are potent triggers of inflammation and may thus participate to the development/progression of CAVS through a specific NF-κB signature. Studies using a Mendelian randomization approach have underlined that the apolipoprotein B (apoB)-containing lipoproteins, low-density lipoprotein (LDL) and Lp(a), are possibly causally related to CAVS.[8–10] The circulating level of oxidized phospholipid (OxPL), a component of oxidized LDL (OxLDL), is independently related to the progression rate of CAVS.[11] We reported that the enzymes lipoprotein-associated phospholipase A2 (Lp-PLA2) and autotaxin (ATX), a lysophospholipase D, are overexpressed in surgically explanted stenotic aortic valves.[12,13] During the oxidation of LDL, OxPLs are converted into lysophosphatidylcholine (LysoPC) by Lp-PLA2.[14] On the other hand, oxidation of LDL also generates significant amount of lysophosphatidic acid (LPA),[15] a bioactive lipid that accumulates in mineralized, stenotic aortic valves.[13] ATX transforms LysoPC into LPA and its activity is enriched in isolated Lp(a) fraction.[13] In this work, we hypothesized that OxLDL-derived LPA promotes the progression of CAVS through a NF-κB-induced osteogenic program unresponsive to the negative regulation of IκBα.

2. Methods

Expanded methods are in the online supplement.

2.1 Procurement of tissues for analyses

We examined stenotic aortic valves (CAVS) that were explanted from patients at the time of aortic valve replacement. Control non-calcified aortic valves with normal echocardiographic analyses were obtained during heart transplant procedures. The protocol and experiments detailed in the method section were approved by the IUCPQ ethical committee and informed consent was obtained from the subjects. The study conforms with the declaration of Helsinki.

2.2 Isolation of LDL

LDLs were freshly isolated from healthy human donors by sequential ultracentrifugation.

2.3 VIC isolation and culture

VICs were isolated and purity of the cell preparation was confirmed as previously described.[16] Cells were used between passage 4–7 and were incubated for 7 days with a mineralizing medium (NaH_2PO_4, 2 mM) as previously described.[17]

2.4 Real-time polymerase chain reaction

Total RNA was isolated with RNeasy micro kit from Qiagen (ON, Canada). One microgram of RNA was reverse transcribed using the Quantitec Reverse Transcription Kit from Qiagen. Quantitative real-time PCR (qPCR) was performed with Quantitec SYBR Green PCR kit from Qiagen on the Rotor-Gene 6000 system (Corbett Robotics Inc., CA, USA).

2.5 Luciferase reporter assay

COS7 and VICs were transfected with the PathDetect NF-kB cis Reporting System (Agilent, CA, USA) or BMP2 promoter (Addgene, MA, USA) fused to firefly luciferase gene along with a vector encoding for the renilla luciferase (Promega, WI, USA) as a reporter for transfection efficiency.

2.6 Immunofluorescence on cells

Incubation with antibodies against LPAR1 (Novus Biologicals, ON, Canada) was performed in PBS1X containing 1% milk overnight at 4 °C. Cells were incubated 1 h with alexa568-conjugated secondary antibodies and with alexa488-conjugated phalloidin (Molecular Probes/ThermoFisher Scientific, ON, Canada). Confocal images were acquired using a Zeiss microscope Axio Observer Z1, LSM800 driven by the Zen software (Objective 40× oil, 1.4 NA, Zeiss, ON, Canada).

2.7 Quantitative chromatin immunoprecipitation

Cells were treated for 6 h with LPA and were then cross-linked in 1% formaldehyde solution (Sigma, ON, Canada) for 15 min at room temperature. Cells were washed twice with PBS1X and harvested in 1 mL of PBS1X containing protease inhibitor cocktail (PIC) (Sigma, ON, Canada). Following centrifugation, pellets were resuspended and sonicated to shear the DNA to an average length of 200–800 base pairs. Antibodies against p65 (BioVision, CA, USA) or p65 phosphoS536 or non-relevant rabbit IgG (Cell Signaling Technology, MA, USA) antibodies were incubated with proteins G dynabeads (Life technologies, ON, Canada). Samples were washed first with low salt wash buffer, then with high salt wash buffer, followed with LiCl wash buffer and finally with TE buffer at 4 °C . The complex was then eluted from dynabeads by adding 210 µL of elution buffer at 65 °C for 1 h. The eluted samples were reverse cross-linked by adding 8 µL of 5 M NaCl and incubated at 65 °C overnight. DNA fragments were purified by using phenol-chloroform and samples were analysed by qPCR.

2.8 Animals

All animal protocols were conducted according to guidelines set out by the Laval University Animal Care and Handling Committee and are conform with the NIH guidelines for the care and use of laboratory animals. Male $LDLR^{-/-}$/$ApoB^{100/100}$/IGF2 (on C57Bl/6J background) (established colony) were housed in a pathogen-free, temperature-controlled environment under a 12:12 h light–dark cycle and fed *ad libitum* of a high fat, high sucrose, cholesterol diet (55% calories from fat, 28% from sucrose, 0.2% cholesterol) for 9 months starting at 12 weeks of age. At the end of protocol, mice were sacrificed by anaesthesia under isoflurane (2–3% inhalation) and cardiac puncture, which was performed by a qualified technician.

2.9 Echocardiography in mice

Transthoracic echocardiography was performed under 2.5% isofluorane anaesthesia, with a L15-7io (5–12 MHz) and S12-4 (4–12 MHz) probes connected to a Philips HD11XE ultrasound system (Philips Healthcare Ultrasound, Netherlands).

2.10 Statistical analyses

Continuous data were expressed as mean ± SEM. Continuous data were tested for normality of distribution with the Shapiro–Wilk test and compared with Student's *t*-test. For continuous data with a non-normal distribution or with a $n \leq 10$ the values were compared between groups with non-parametric Wilcoxon–Mann–Whitney or Kruskal–Wallis test when two or more than two groups were compared respectively. Post hoc Steel–Dwass multiple comparisons test were performed when the *P* value of the Kruskal–Wallis test was <0.05. In mice, changes in transaortic velocities between 6 and 9 months were compared with paired *t*-test. Categorical data were expressed as percentage and compared with Fischer's exact test. For *in vitro* experiments with VICs, n represents the number of experiment performed with different donors. A *P*-value < 0.05 was considered significant. Statistical analysis was performed with a commercially available software package JMP 12.0 or Prism 6.0.

3. Results

3.1 OxLDL-induced osteogenic program in VICs is mediated by LPA

Human VICs were obtained from non-mineralized aortic valves (heart transplantation; see Supplementary material online, *Table S1*) and treated with a mineralizing medium for 7 days.[18] VIC cultures treated with OxLDL (100 ng/mL) (copper-treated LDL isolated from healthy donors; see Supplementary material online, *Table S2*) increased the deposition of calcium, which was determined by the Arsenazo III method, by 2.7-fold (*Figure 1A*). However, the addition of Ki16425, an inhibitor of LPA receptor 1 (LPAR1/Edg-2) and LPAR3/Edg-7, to the growth medium of VIC cultures prevented OxLDL-induced mineralization (*Figure 1A*). These data suggested that LPA produced by OxLDL promoted the mineralization of VICs. We next assessed the effect of LPA (10 μM) with different acyl chain length and saturation on the mineralization of VICs. We found that the level of mineralization increased with the acyl chain length and with non-saturated species (*Figure 1B*). For the next series of experiments we used LPA18:1 as it is present in different bodily fluids. Different doses of LPA were used in mineralization assay with VICs. We observed that mineralization of VIC cultures increased and plateaued between 1 μM and 5 μM of LPA, whereas a dose of 10 μM was more potent (*Figure 1C*). Since the level of LPA in different tissues is in the low micromolar range, we next used 10 μM of LPA18:1 for follow-up experiments.[19] To examine whether LPA promoted the mineralization of VIC cultures through an osteogenic process we measured the levels of bone-related markers in cells treated for 7 days with LPA. VICs treated with LPA had higher level of transcripts encoding osteogenic markers *RUNX2*, *BGLAP*, *COL1A1*, and *BMP2* (*Figure 1D–G*). Also, the activity of alkaline phosphatase (ALP), an osteogenic marker, increased by 1.8-fold following a treatment with LPA for 7 days (*Figure 1H*). Bone morphogenetic protein 2 (BMP2) is a potent morphogen involved in osteogenic differentiation. By using noggin, a natural inhibitor of BMPs, we observed that LPA-induced mineralization of VIC cultures was abrogated (*Figure 1I*). Small interfering RNA for *BMP2* reduced significantly the mRNA and protein levels of the target (see Supplementary material online, *Figure S1A* and *B*) and prevented LPA-induced mineralization of VICs (*Figure 1J*).

3.2 LPA induces an osteogenic program in VICs through LPAR1

Considering that OxLDL-mediated mineralization was abrogated by Ki16425, an inhibitor of LPAR1 and LPAR3, we next assessed the gene expression profile of *LPAR1* and *LPAR3* in VICs. We documented that mRNA encoding for *LPAR1* was robustly expressed by VICs, whereas *LPAR3* was not detected (*Figure 2A*). Examination by immunofluorescence and confocal microscopy showed in isolated VICs that LPAR3 was not expressed (see Supplementary material online, *Figure S2*), whereas LPAR1 was expressed in both the cytosol and at the cell membrane, which was delimited by membrane-associated cortical F-actin shown with phalloidin (*Figure 2B* and see Supplementary material online, *Figure S2*). Small interfering RNA for *LPAR1* decreased significantly the gene and protein levels of the target (see Supplementary material online, *Figure S3A* and *B*) and prevented OxLDL- and LPA-induced mineralization of VIC cultures (*Figure 2C*). A knockdown LPAR1 in VICs prevented the rise of *BMP2* mRNA measured 24 h after a treatment with LPA (*Figure 2D*). Similarly, LPA-induced rise of *RUNX2*, *BGLAP* and *COL1A1* (measured at 24 h) was abrogated by a knockdown of LPAR1 in VICs (*Figure 2E–G*). We assessed the expression level of LPAR1 in human surgically explanted CAVS and control non-mineralized aortic valves obtained from heart transplantations (see Supplementary material online, *Table S3*). The level of *LPAR1* mRNA was increased by 1.5-fold in human CAVS tissues when compared with control non-mineralized aortic valves (*Figure 2H*). Both mineralized tricuspid and bicuspid aortic valves had higher levels of *LPAR1* mRNA compared with control valves (see Supplementary material online, *Figure S4*). By using western blotting we documented that LPAR1 was increased by 5.2-fold in human mineralized aortic valves (*Figure 2I*). With immunofluorescence and confocal microscope imaging, we found in mineralized, stenotic aortic valves that LPAR1 was co-expressed with vimentin, a marker of VICs (*Figure 2J* and see Supplementary material online, *Figure S5*), whereas LPAR3 was not expressed (see Supplementary material online, *Figure S5*). LPAR1 has been shown to potently stimulate RhoA/Rho kinase (ROCK) pathway in different cell populations,[20] but whether VICs respond in a similar manner has not been explored. In isolated VICs, we found that LPA rapidly induced the activity of ROCK, which was already detected after 15 min of treatment (*Figure 2K*). The silencing of LPAR1 in VICs abrogated the activation of ROCK induced by LPA (measurements performed at 30 min; *Figure 2L*). The inhibition of ROCK with Y27632 (*Figure 2M*) prevented LPA-induced mineralization of VIC cultures (*Figure 2N*). These data thus suggest that LPAR1 is coupled to RhoA/ROCK in promoting the mineralization of cell cultures and the osteogenic differentiation of VICs.

3.3 LPA-mediated activation of RhoA/ROCK promotes NF-κB activity

RhoA/ROCK may activate NF-κB to induce mineralization of VIC. To verify this hypothesis we transfected the fibroblast cell line COS7 with a luciferase vector containing κB responsive elements and we treated cell cultures with LPA. LPA activated the κB responsive element at 1 h with a maximal response at 6 h (*Figure 3A*). This experiment was replicated in human VICs and showed that LPA increased after 6 h the activity of a reporter vector containing κB responsive elements (see Supplementary

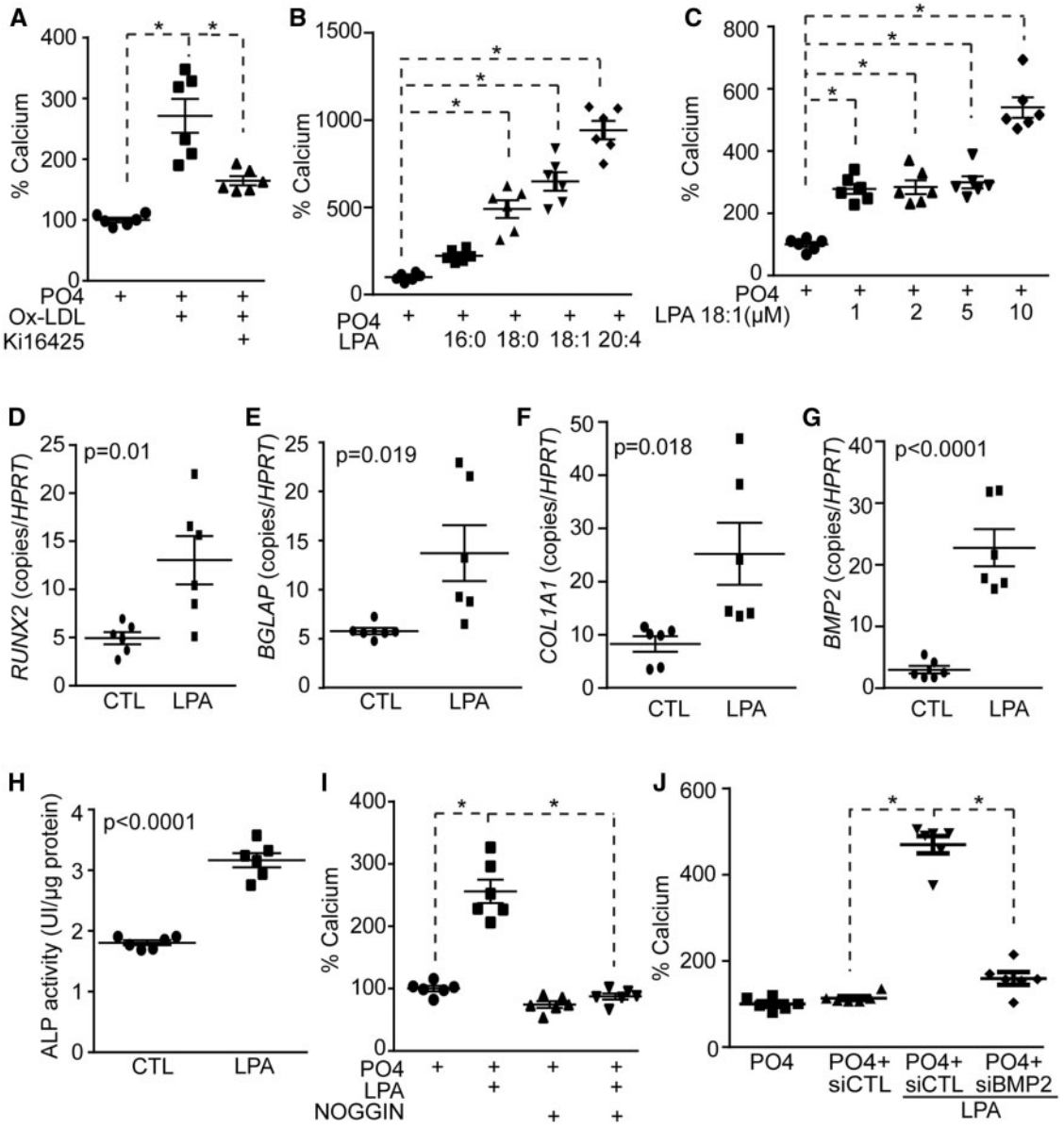

Figure 1 LPA-mediated VIC mineralization depends on BMP2. (*A*) Treatment with Ki16425 prevents OxLDL-induced mineralization of VICs ($n = 6$) (calcium measured after 7 days). (*B*) VICs were treated with mineralizing medium in presence of different LPA species ($n = 6$). (*C*) VICs were treated with mineralizing medium in presence of increasing LPA 18:1 concentration ($n = 6$). (*D–H*) RUNX2, BGLAP, COL1A1, BMP2 genes ($n = 6$) and ALP activity ($n = 6$) were increased in VICs following LPA treatment (7 days). (*I*) Treatment with Noggin inhibits LPA-induced mineralization ($n = 6$). (*J*) BMP2 siRNA abrogates LPA-induced mineralization of VICs ($n = 6$). Values are mean ± SEM. OxLDL: 100 ng/mL, Ki16425: 10 μM, LPA: 10 μM, Noggin: 2.5 μM. * $P < 0.05$.

material online, *Figure S6*). In the next series of experiments, the reporter assay was thus conducted at 6 h after stimulation with LPA. Increased κB activity in reporter assay following a treatment with LPA was prevented when BAY11-7085, an inhibitor of IκB kinase (IKK), was added to the growth medium (*Figure 3B*). Also, in mineralization assay over 7 days, BAY11-7085 prevented the mineralization of VIC cultures induced by LPA (*Figure 3C*), indicating that the process possibly relied on the NF-κB pathway. Following an inhibition of RhoA/ROCK with Y27632 we noted that LPA-induced κB reporter activity was abrogated (*Figure 3D*). To confirm the role of RhoA in the activation of the NF-κB pathway we next used a vector encoding for a dominant negative RhoA mutant N19 (RhoAN19). COS7 were co-transfected with RhoAN19 and the κB reporter coupled to luciferase. A co-transfection of the dominant negative RhoAN19 mutant prevented the LPA-induced activation of κB reporter (*Figure 3E*). Also, the co-transfection of a constitutively active RhoA mutant (RhoAL63) in COS7 induced the activation of the κB luciferase reporter (*Figure 3F*). To buttress these findings, we measured the level of *IL6* mRNA, a NF-κB responsive gene, following stimulation with LPA in presence or absence of Y27632, an inhibitor of RhoA/ROCK. A treatment during 24 h with LPA in VICs resulted in a significant increase of *IL6* mRNA level (*Figure 3G*). The addition of Y27632 to the growth medium of VIC cultures prevented the rise of *IL6* mRNA induced by

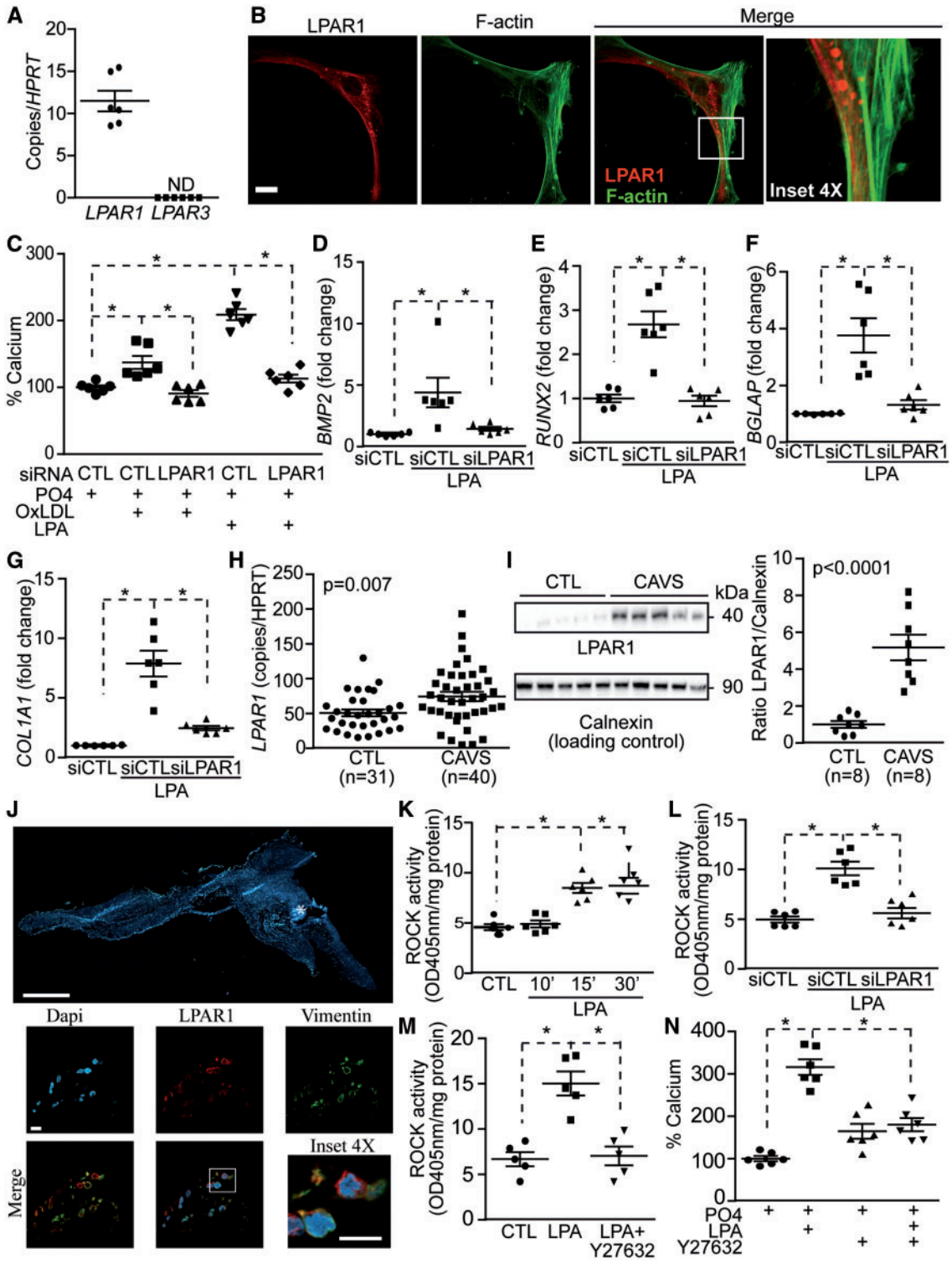

Figure 2 LPAR1 mediates LPA response in VICs. (*A*) *LPAR1* expression in VICs ($n = 6$). (*B*) Confocal images of LPAR1 in VICs. Scale bar 20 μM, ($n = 5$). (*C*) LPAR1 is required for OxLDL and LPA induced mineralization of VICs ($n = 6$). (*D–G*) siLPAR1 prevented LPA-mediated rise of *BMP2* (*D*), *RUNX2* (*E*), *BGLAP* (*F*) and *COL1A1* (*G*) ($n = 6$) (measurements at 24 h). (*H*) LPAR1 mRNA measurement in control non-mineralized (CTL) ($n = 31$) vs. calcified aortic valves (CAVS) ($n = 40$). (*I*) Representative western blot and quantification of LPAR1 in CTL ($n = 8$) vs. CAVS ($n = 8$). (*J*) Epifluorescence image of a calcified aortic valve showing the organization of the tissue in DAPI, scale bar 1000 μM and confocal images showing LPAR1 and vimentin co-expression in the same tissue, scale bar 10 μM ($n = 10$). (*K–M*) ROCK activity measurements; kinetics following LPA treatment ($n = 6$) (*K*), siLPAR1 negated LPA response ($n = 6$) (*L*) and Y27632 abrogated LPA effect ($n = 5$) (*M*). (*N*) Treatment with Y27632 reduces LPA-mediated mineralization in VICs ($n = 6$). Values are mean ± SEM. LPA: 10 μM, OxLDL: 100 ng/mL, Y27632: 5 μM; * $P < 0.05$.

LPA (*Figure 3G*). LPA-induced rise of *IL6* mRNA in VICs was abrogated by a knockdown of LPAR1 (*Figure 3H*).

3.4 LPA-induced expression of BMP2 is mediated by RhoA and NF-κB

Given that BMP2 plays an important role in LPA-induced osteogenic reprogramming of VICs, we next evaluated whether BMP2 is activated through a RhoA-NF-κB pathway. A vector encoding for the promoter region of *BMP2* and coupled with the luciferase gene was transfected in COS7 cells to assess its activity in response to LPA. We observed that LPA activated the promoter region of *BMP2* with a maximal response after 6 h (*Figure 4A*). This experiment was also replicated in human VICs and showed that after 6 h LPA activated a reporter vector containing the *BMP2* promoter region (see Supplementary material online, *Figure S7*). After 24 h of treatment with LPA, the level of BMP2 protein, assessed with an ELISA, was significantly increased in VIC cultures (*Figure 4B*). In reporter assay, LPA-induced activity of *BMP2* promoter was prevented by a co-transfection with the dominant negative RhoA mutant vector (RhoAN19; *Figure 4C*). In VICs, Y27632 (inhibitor of ROCK) significantly reduced LPA-induced rise of *BMP2* transcripts measured at 24 h (*Figure 4D*). The inhibition of NF-κB pathway with BAY11-7085 also prevented LPA-induced rise of *BMP2* mRNA at 24 h (*Figure 4D*). To further show an involvement of NF-κB in the activation of *BMP2* we next silenced p65 with small interfering RNA. A knockdown of p65 (see Supplementary material online, *Figure S8A* and *B*) significantly reduced the level of *BMP2* transcripts measured at 24 h after a treatment with LPA (*Figure 4E*). Also, a silencing of p65 prevented the mineralization of VIC cultures induced by LPA over 7 days (*Figure 4F*). These data thus suggested that RhoA and p65 subunit of NF-κB positively regulates the expression of *BMP2* and promotes the mineralization of VIC cultures.

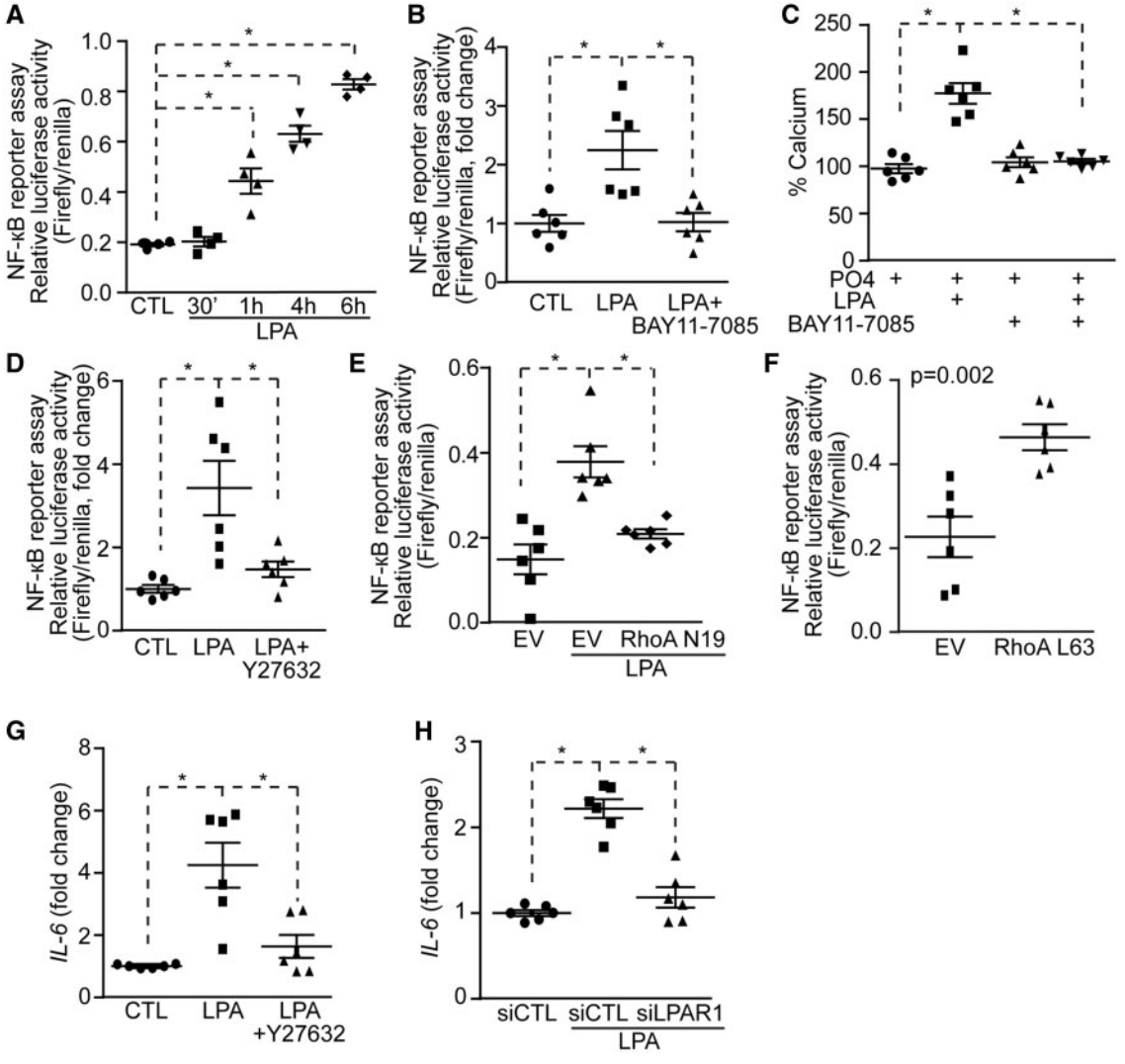

Figure 3 LPA-induced VICs mineralization relies on the NF-κB pathway. (*A* and *B*) NF-κB reporter assay showing increased NF-κB activity in response to LPA ($n = 4$) (*A*) and its inhibition by BAY11-7085 ($n = 6$) (*B*). (*C*) BAY11-7085 prevents LPA-induced mineralization ($n = 6$). (*D–F*) NF-κB reporter assay; Y27632 ($n = 6$) (*D*) and RhoA N19 ($n = 6$) (*E*) inhibits and RhoA L63 ($n = 6$) (*F*) mimics LPA effect on NF-κB activity. (*G* and *H*) *IL-6* mRNA measurements in response to LPA, Y27632 ($n = 6$) (*G*) and siLPAR1 ($n = 6$) (*H*) decreases LPA-induced IL-6 rise. Values are mean ± SEM. LPA: 10 μM, BAY11-7085: 5 μM, Y27632: 5 μM; * $P < 0.05$.

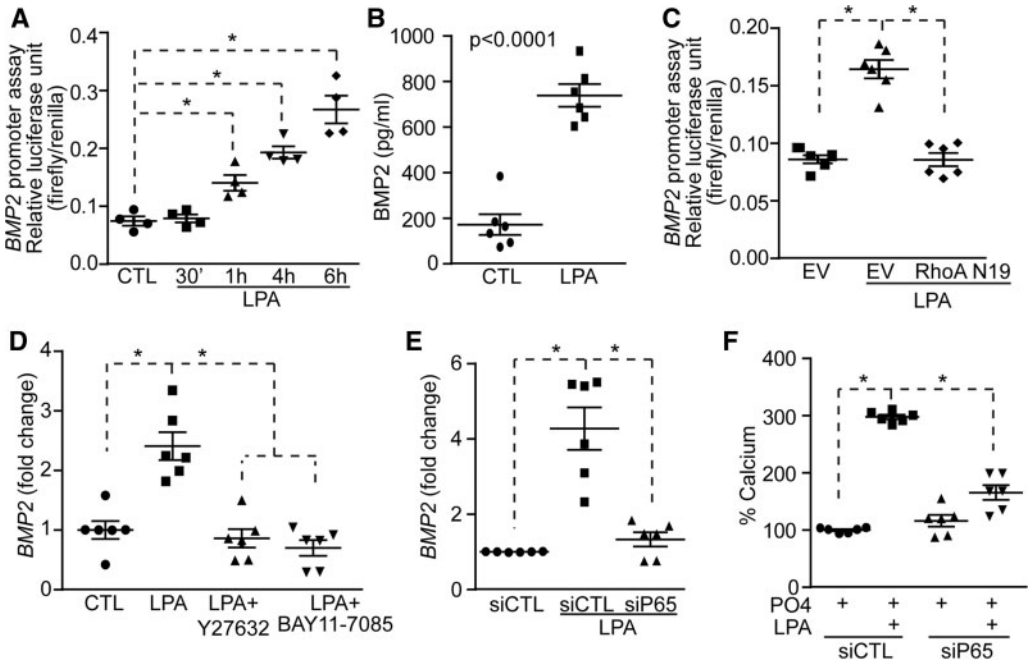

Figure 4 LPA-mediated activation of the NF-κB pathway promotes BMP2 expression. (*A* and *B*) LPA increases *BMP2* promoter activity ($n = 4$) (*A*) and BMP2 protein level ($n = 6$) (*B*). (*C*) RhoA N19 inhibits LPA-induced *BMP2* promoter activity ($n = 6$). (*D*) Y27632 ($n = 6$) and BAY11-7085 ($n = 6$) abrogates LPA-mediated rise in *BMP2* mRNA. (*E* and *F*) p65 is required for LPA regulation of *BMP2* level ($n = 6$) (*E*) and mineralization ($n = 6$) (*F*). Values are mean ± SEM. LPA: 10 μM, Y27632: 5 μM, BAY11-7085; * $P < 0.05$.

3.5 Phosphorylation of serine 536 of p65 promotes an osteogenic program not responsive to the negative feedback exerted by IκBα

The human *BMP2* promoter contains two putative κB consensus sites [NRE1 (-354/-344 bp) and NRE2 (-2548/-2538 bp)] (*Figure 5A*). To substantiate that *BMP2* is a target of NF-κB we performed quantitative chromatin immunoprecipitation assay (qChIP) in VICs using an antibody directed against p65. Treatment with LPA for 6 h induced p65 recruitment to the NRE1 site of *BMP2* and also to the promoter region (-136/-126 bp) of *IL6*, which was used as a positive control (*Figure 5B* and *C*). Attempt to perform qChIP for the distal (-2548/-2538 bp) κB site (NRE2) in *BMP2* promoter region was unsuccessful owing to its high CG content. IκBα negatively regulates the expression of genes following activation of NF-κB. IκBα is induced by p65 and shuttles between the cytosol and the nucleus where it exerts a negative control over the binding of p65 to gene promoters. However, some gene promoters (e.g. *IL8*) that bind to p65 when phosphorylated on serine 536 (p65 pS536) are not sensitive to the negative regulation induced by IκBα.[4] In order to examine whether *BMP2* is not sensitive to the negative regulation of IκBα we used the fungal-derived toxin leptomycin B, which inhibits the nuclear export and increases the level of IκBα in the nucleus of cells.[4] To verify the efficacy of leptomycin B we performed western blotting for IκBα following cell fractionation. Nuclear fraction of VICs was positive for the nuclear histone H3 and negative for the cytosolic marker Golgin-97, indicating an adequate cell fractionation (*Figure 5D*). The treatment with leptomycin B increased nuclear level of IκBα, whereas it decreased the cytosolic content of IκBα (*Figure 5D* and *E*). VICs were next treated with LPA with or without leptomycin B for 24 h and *IL6*, *IL8*, and *BMP2* mRNAs were measured. Leptomycine B prevented LPA-induced rise of *IL6* (*Figure 5F*), a gene known to be sensitive to IκBα.[4] However, leptomycin B did not affect LPA-induced expression of *IL8* and *BMP2* (*Figure 5G* and *H*). To further corroborate this finding we treated VICs with a mutant IκBα SS32-36AA vector, which cannot be phosphorylated and is thus acting as a super repressor. Similarly to leptomycin B the mutant IκB super repressor did not impact on LPA-induced expression of *BMP2* and *IL8*, whereas it prevented the rise of *IL6* mRNA (*Figures 5I–K*). In addition, transfection of VICs with IκB super repressor did not prevent LPA-induced mineralization of cell cultures (*Figure 5L*). Taken together, these data suggested that LPA-induced activation of *BMP2* expression relies possibly on p65 pS536. In reporter assay for the *BMP2* promoter, a transfection of COS7 cells with a vector encoding for a dominant negative p65 S536A, which cannot be phosphorylated on serine 536, abrogated LPA-induced *BMP2* promoter activity (*Figure 6A*). Also, we found that the transfection of a dominant negative p65 S536A vector in VICs reduced significantly the mineralization of cell cultures induced by LPA after 7 days (*Figure 6B*). Conversely, the transfection of a vector encoding for a phosphomimetic of serine 536 p65 (p65 S536E) increased the mineralization of VIC cultures by 1.9-fold, whereas the transfection of vector encoding for wild-type p65 did not modify the level of mineral in cell cultures (*Figure 6C*). In qChIP assay, we found that following a treatment of VICs with LPA for 6 h, p65 pS536 is recruited to the *BMP2* promoter whereas it is not recruited to the promoter region of *IL6* (*Figure 6D* and *E*). These data suggested that LPAR1 is coupled to RhoA in activating p65 pS536, which is recruited to the *BMP2* promoter. To verify this hypothesis we measured by western blotting the level of p65 pS536 in response to LPA. Time-course experiments using VICs revealed that

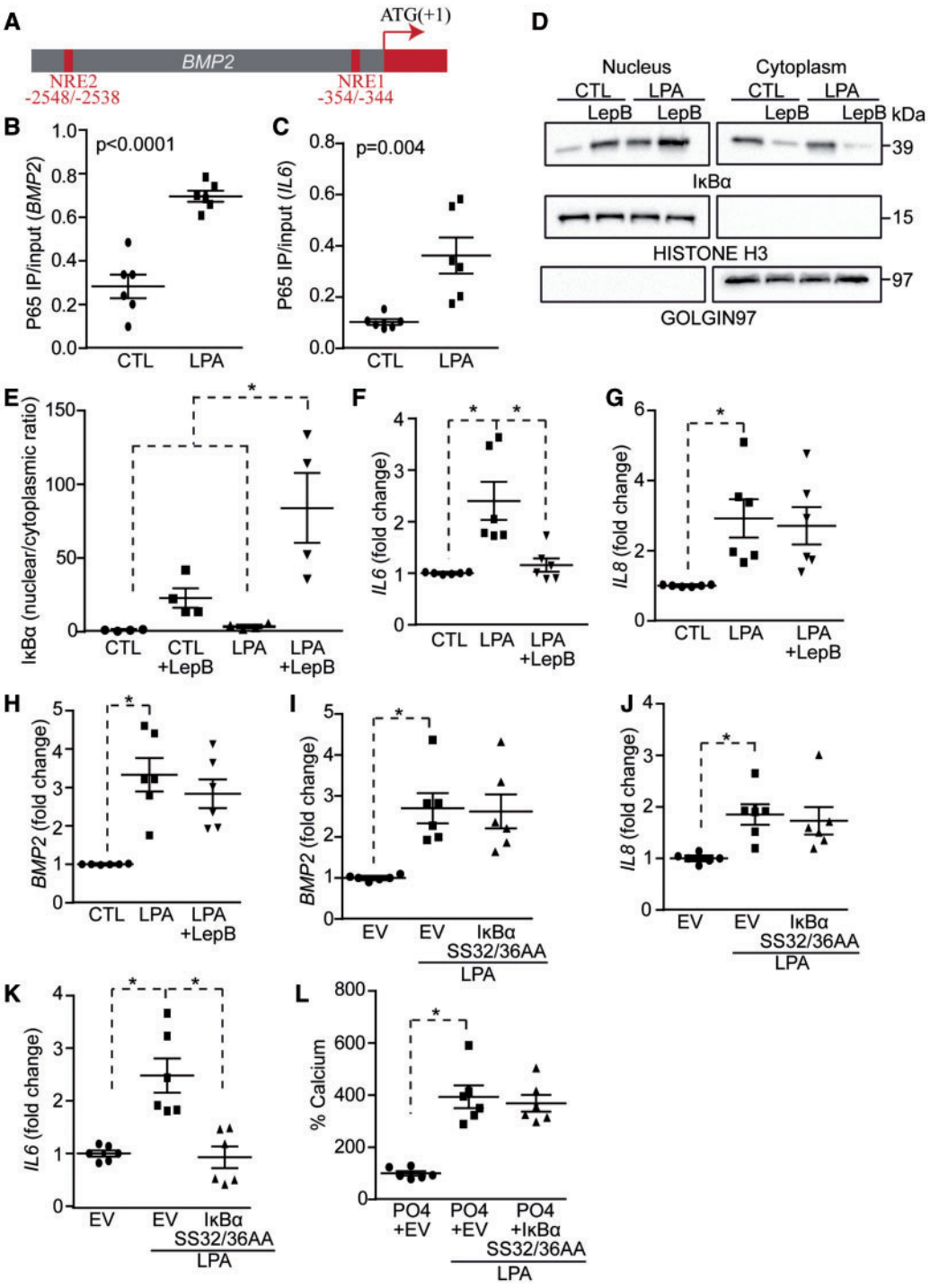

Figure 5 LPA-mediated activation of the NF-κB pathway regulates BMP2 promoter activity. (*A*) Scheme depicting NRE sites localization in the *BMP2* promoter. (*B* and *C*) ChIP assays; p65 binds to *BMP2* (*B*) and *IL6* (*C*) promoters in response to LPA ($n = 6$). (*D* and *E*) Western blots on nuclear and cytoplasmic fractions demonstrating the efficiency of leptomycinB (LepB) treatment (*D*); quantification of WB ($n = 4$) (*E*). (*F–H*) LepB inhibits LPA-mediated rise of *IL6* (*F*) but not of *IL8* (*G*) nor *BMP2* (*H*) ($n = 6$). (*I–K*) IκBα super repressor (SS32/36AA) does not block LPA effect on *BMP2* (*I*) and *IL8* (*J*), but blocks its effect on *IL6* (*K*) ($n = 6$). (*L*) IκBα SS32/36AA has no effect on LPA-induced mineralization of VICs ($n = 6$).Values are mean ± SEM. LPA: 10 μM, Leptomycin B: 20 nM; * $P < 0.05$.

LPA rapidly activated the phosphorylation of serine 536 on p65 with a sustained response, which gradually increased from 15 to 60 min (*Figure 6F*). Inhibition of ROCK with Y27632 negated LPA-induced phosphorylation of p65 S536 (*Figure 6G*). In human aortic valves, we found by western blotting that the p65 pS536/p65 ratio was increased by 4.6-fold in CAVS compared with control non-mineralized aortic valves (*Figure 6H*). IKKα and IKKβ are known to act downstream of RhoA/ROCK in phosphorylating p65.[21] We thus silenced IKKα or IKKβ (see

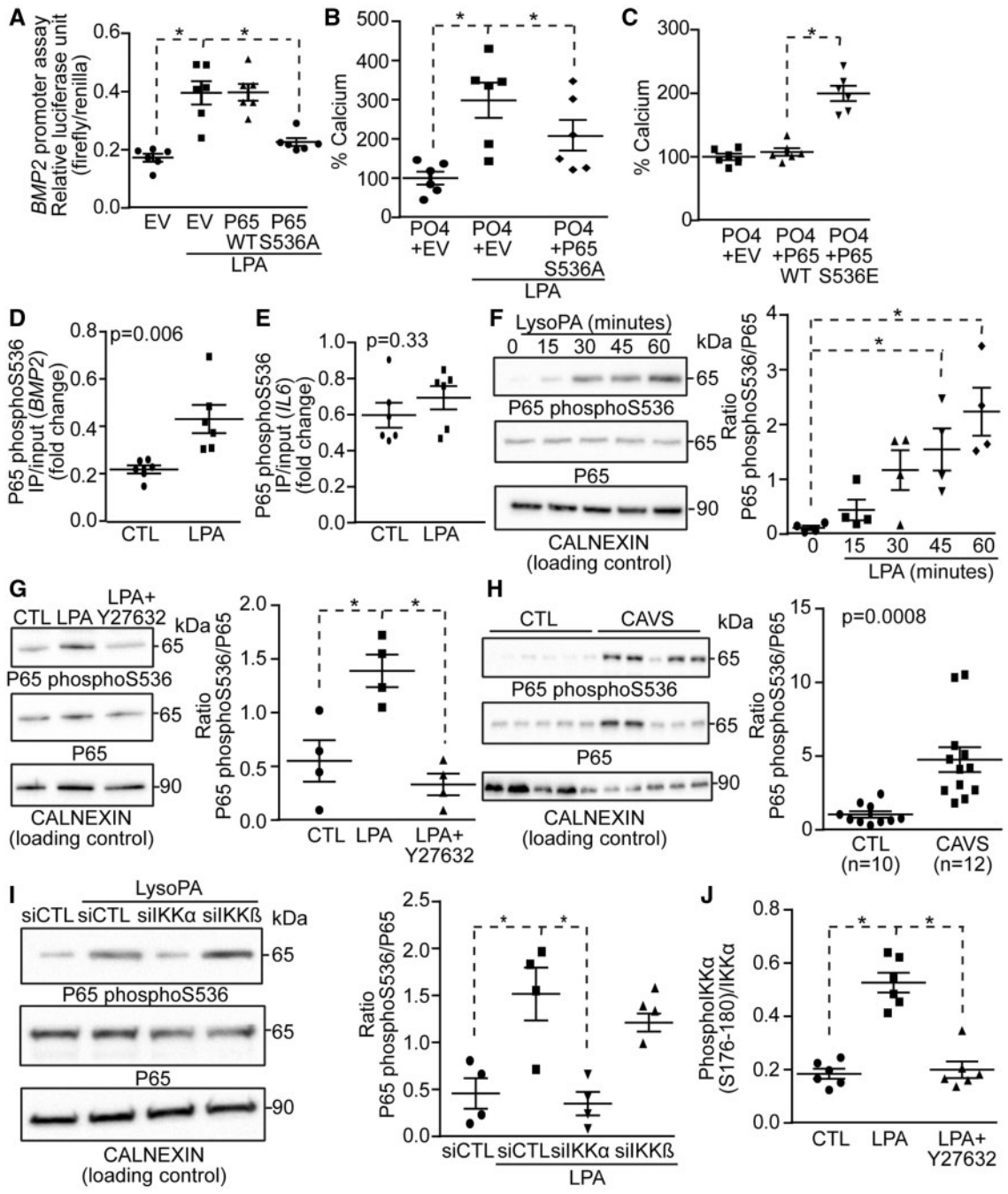

Figure 6 LPA-mediated activation of BMP2 relies on phosphorylation of p65 S536. (*A–C*) P65 S536A inhibits LPA-mediated rise in *BMP2* promoter activity ($n = 6$) (*A*) and mineralization ($n = 6$) (*B*), while p65 S536E mimics the effect of LPA ($n = 6$) (*C*). (*D–E*) ChIP assays; p65 phosphoS536 binds to *BMP2* (*D*), but not to *IL6* (*E*) promoters in response to LPA ($n = 6$). (*F*) LPA induces p65 phosphorylation on S536 ($n = 4$). (*G*) Y27632 blocks LPA-induced p65 S536 phosphorylation ($n = 4$). (*H*) Representative western blot showing that p65 phosphoS536 is increased in CAVS ($n = 12$) vs. control ($n = 10$) tissues. (*I*) p65 S536 phosphorylation relies on IKKα ($n = 4$). (*J*) LPA-mediated IKKα phosphorylation is abrogated by Y27632 ($n = 6$). Values are mean ± SEM. LPA: 10 μM; * $P < 0.05$.

Supplementary material online, *Figure S9A* and *B*) and we documented the level of p65 pS536 in response to LPA in VICs. The knockdown of IKKα but not of IKKβ negated LPA-induced phosphorylation of p65 on S536 (*Figure 6I*). In the same line, phosphorylation of IKKα on S176-180 was increased after LPA treatment of VICs, whereas the inhibition of ROCK with Y27632 prevented this effect (*Figure 6J*). These data thus indicate that LPA-mediated activation of RhoA/ROCK entrains the activity of IKKα whereby p65 is phosphorylated on S536 and promotes the expression of BMP2, which directs an osteogenic response in VICs.

3.6 Inhibition of Lpar1 slows the progression of CAVS in a mouse model

LDLR$^{-/-}$/ApoB$^{100/100}$/IGFII transgenic mice (IGFII) under a high-fat and high-sucrose (HF–HS) diet develop CAVS.[22] compared with C57BL/6 mice (same background of IGFII mice) the serum level of LPA was increased significantly in IGFII mice under HF–HS diet for 6 months and correlated with ATX activity ($r^2 = 0.79$, $P = 0.005$) and cholesterol levels ($r^2 = 0.50$, $P = 0.02$; *Figure 7A–C*). Similarly to human CAVS, we documented a significant rise of *Lpar1* mRNA in the aortic root (aortic valve plus aortic wall of the root) of IFGII mice when compared with control C57BL/6 mice (*Figure 7D*). Noteworthy, isolated mouse VICs expressed *Lpar1* but not *Lpar3* mRNAs (see Supplementary material online, *Figure S10*). The level of *Lpar1* mRNA was positively correlated with *Bmp2* mRNA level ($r^2 = 0.97$, $P < 0.0001$; *Figure 7E*). To mimic the clinical setting where patients are treated with an ongoing disease process, we next assessed whether the administration of Ki16425 (Lpar 1-3 blocker) may decrease the progression rate of CAVS in IGFII mice with an established and ongoing disease. Treatments were thus started after 6 months of HF–HS diet when the transaortic velocities were significantly increased compared with the baseline values (165.9 ± 2.6 cm/s vs. 102.9 ± 2.4 cm/s, $P < 0.0001$; see Supplementary material online, *Table S4*). Mice were treated with Ki16425 (5 mg/kg/d i.p.)[23] or vehicle for the next 3 months while the HF–HS diet was maintained (*Figure 7F*). Transaortic velocities at 6 months were similar between the vehicle- and Ki16425-treated IGFII mice (163.1 ± 3.0 cm/s vs. 168.0 ± 4.2 cm/s, $P = 0.35$). In the next three months (from 6 to 9 months), the transaortic velocities increased significantly in control IGFII mice receiving the vehicle (163.1 ± 3.0 cm/s vs. 186.4 ± 5.9 cm/s, $P = 0.0007$ respectively at 6 and 9 months; *Figure 7G*; see Supplementary material online, *Tables S5* and *S6*). In the IGFII mice receiving Ki16425, there was a non-significant rise in transaortic velocity between 6 and 9 months (168.0 ± 4.2 cm/s vs. 175.9 ± 5.7 cm/s, $P = 0.18$ respectively at 6 and 9 months) and 5/11 (45%) mice showed a decrease or no progression of transaortic velocities during this period (*Figure 7H*; see Supplementary material online, *Tables S5* and *S6*). The delta transaortic velocity (transaortic velocity at 9 months – transaortic velocity at 6 months) was decreased by approximately three-fold in IGFII mice treated with Ki16425 compared with control mice receiving the vehicle (+7.9 ± 5.6 cm/s vs. +23.3 ± 5.1, $P = 0.02$ respectively for Ki16425 and control; *Figure 7I*). Also, Ki16425-treated mice showed a significant improvement in the left ventricular fractional shortening (LVFS), whereas it was not significantly modified in the control IGFII mice receiving the vehicle (delta LVFS 9–6 months: +7.9 ± 2.2 vs. +2.3 ± 1.5, $P = 0.04$ respectively for Ki16425 and control; *Figure 7J*). We next performed post-mortem examination of aortic valves to document the osteogenic activity by measuring the intensity of a near-infrared fluorescent probe that recognizes hydroxyapatite of calcium (OsteoSense 680EX). Compared with control IGFII mice receiving the vehicle, the administration of Ki16425 reduced significantly the deposition of hydroxyapatite of calcium in aortic valve leaflets (*Figure 7K*). The cholesterol and triglyceride levels were not affected by a treatment with Ki16425 (see Supplementary material online, *Table S7*).

4. Discussion

In this work, we identified LPAR1 as being involved in the osteogenic effect of OxLDL-LPA. Signalling through p65 pS536 defined an osteogenic signature in the aortic valve by promoting the expression of BMP2 (*Figure 7L*). Inhibition of this pathway by the blockade of Lpar1 in mice decreased the progression rate of CAVS by approximately three-fold.

4.1 OxLDL, LPA, and CAVS

Previous work suggested that oxidative transformation of lipoproteins may play a role in CAVS.[24] Circulating level of OxLDL has been associated with the fibrocalcific remodelling score of surgically explanted stenotic aortic valves.[25] In explanted stenotic, mineralized aortic valves, immunohistological studies have highlighted that apoB, Lp(a), OxLDL and OxPL were present in the vicinity of mineralized nodules.[13,26] Moreover, the intensity of OxLDL staining in explanted mineralized aortic valves is associated with the density of inflammatory cells and the expression of cytokines.[27] Genome-wide transcriptomic analysis has shown an enrichment of inflammatory and osteogenic genes in mineralized, stenotic aortic valves.[28] Also, the presence of dense leucocyte infiltrates, a crude marker of inflammation, in surgically explanted mineralized aortic valves is associated with the fibrocalcific remodelling score.[29] Hence, these data suggest that oxidative transformation of lipoproteins may be involved in inflammation-mediated mineralization of the aortic valve. Recently, a weighted genetic risk score for LDL was found to predict the presence of mineralized aortic valves and CAVS.[8] Also, at the genome-wide level the *LPA* gene variant rs10455872, which strongly predicts the circulating level of Lp(a), was associated with CAVS.[9] These findings raised the possibility that apoB-containing lipoproteins are causally related to CAVS. Previous studies had highlighted that LPA was produced during the oxidation of LDL.[15] In the present work, we highlighted a novel process whereby OxLDL-derived LPA promoted the mineralization of the aortic valve through LPAR1, which was increased in mineralized aortic valves.

4.2 Inflammation and osteogenic transformation of VICs

We found that LPAR1 signalled through RhoA-p65 pS536 and BMP2. The NF-κB pathway exerts a complex and crucial control over inflammation. The NF-κB barcode hypothesis posits that in order to control the expression of large number of genes, which is cell and context dependent, the post-translational modification of NF-κB subunits, namely p65, determines specific programs of gene expression.[30,31] We documented that LPAR1 promoted in VICs the phosphorylation of p65 on serine 536, which triggered the expression of BMP2, a key osteogenic morphogen. We found that p65 pS536, which is not inhibited by IκBα, was increased in explanted mineralized aortic valves. In isolated VICs, p65 pS536 was recruited to the *BMP2* promoter. As p65 pS536 is not responsive to IκBα it is possible that it induces a long-lasting osteogenic effect in the aortic valve. In this regard, the mineralization of VIC cultures induced by LPA was not inhibited by the transfection of a mutant super IκBα repressor. Taken together, these data suggest that LPA derived from OxLDL promotes a NF-κB signature, which is defined by p65 pS536, and promotes an osteogenic program in VICs.

4.3 Progression of CAVS and translational implications

Presently, the treatment of CAVS relies on the replacement of the aortic valve, which can be performed by surgical or catheter-based therapy, in patients with severe, symptomatic aortic stenosis. However, these interventions, often performed in elderly patients with multiple risk factors, carry a substantial morbidity/mortality risk.[32] Hence, the development of a medical therapy would likely result in lesser utilization of resources and

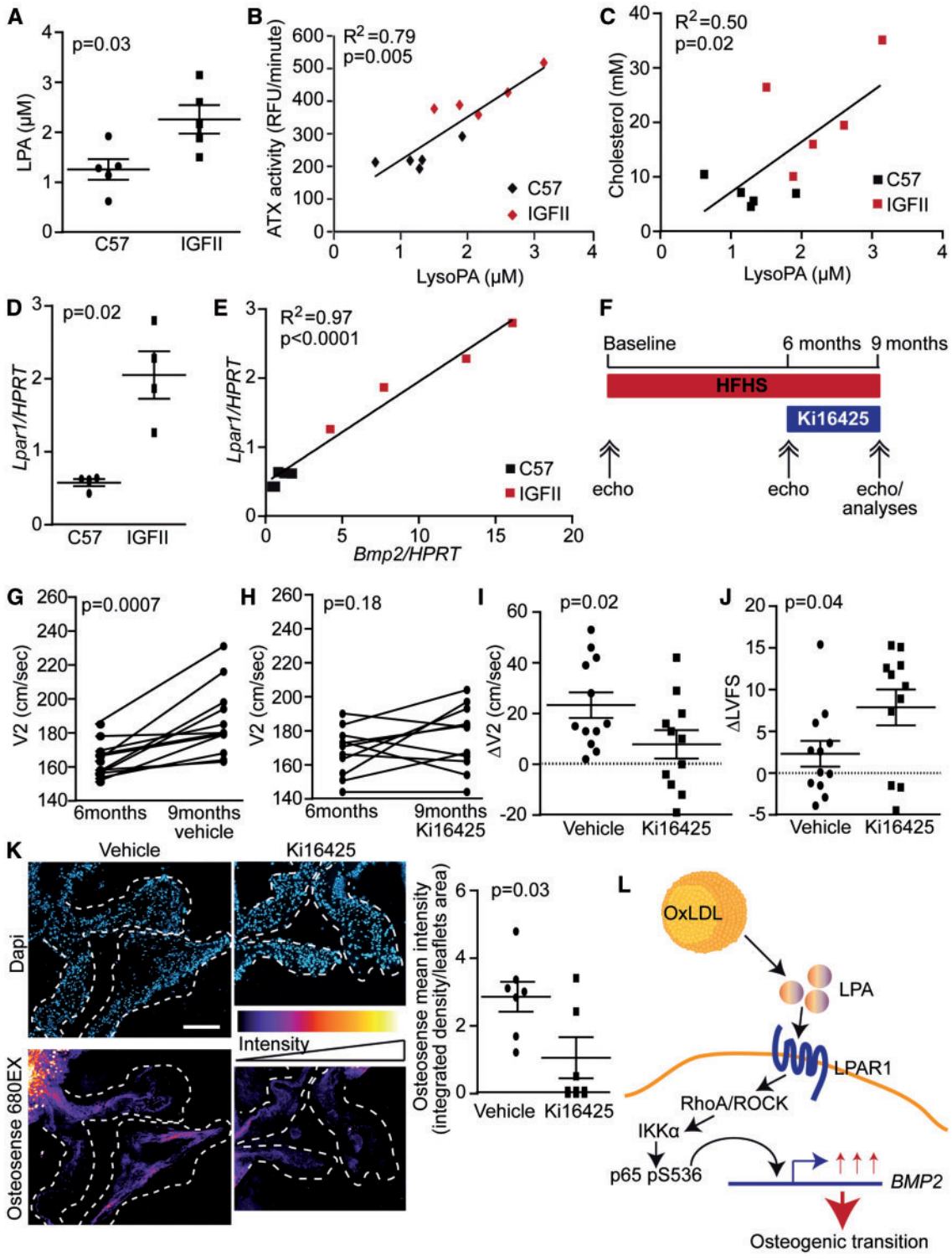

Figure 7 Role of the ATX-LPAR1 pathway *in vivo*. (*A*) LPA is increased in IGFII mice serum ($n = 10$). (*B–C*) LPA level correlates with blood plasma ATX activity (*B*) and cholesterol level (*C*) ($n = 10$). (*D–E*) *Lpar1* is elevated in IGFII mice (*D*) and it correlates with *Bmp2* level (*E*) ($n = 8$). (*F*) Outline of the animal protocol. (*G* and *H*) Transaortic velocities (V2) were increased in mice receiving vehicle (*G*) ($n = 12$) while they were stable in mice receiving Ki16425 (*H*) ($n = 11$). (*I*) ΔV2 was significantly higher in mice receiving vehicle compared with Ki16425 ($n = 23$). (*J*) ΔLVFS was significantly lower in mice receiving vehicle compared with Ki16425 ($n = 23$). (*K*) Hydroxyapatite was more abundant in leaflets of mice receiving vehicle compared with Ki16425 ($n = 13$), scale bar 200 μM. Values are mean ± SEM. Ki16425: 5 mg/kg/day.

better outcomes. From a clinical standpoint, a pharmacotherapy could be started in patients with mild and/or moderate aortic stenosis.[33] However, so far attempts to reduce the progression rate of aortic stenosis have been unsuccessful. Three successive randomized controlled trials have shown that administration of statins, which lowered efficiently LDL cholesterol, failed to show any efficacy on the progression of aortic stenosis.[34] The failure of statins to prevent the progression of CAVS is likely multifactorial and may be linked, at least in part, to the pro-osteogenic effect of this class of drug.[35,36] Also, statins do not appreciably modify the Lp(a) level, a LDL-like particle that contains an apoB linked to apolipoprotein(a).[37] In a murine model of CAVS, we found that circulating levels of LPA were elevated and correlated with ATX activity and cholesterol levels. Similarly to our findings in human mineralized aortic valves the level of *Lpar1* in IGFII mice aortic root (aortic valve and aortic wall) was elevated. The study in mice was carried out as to mimic the clinical setting and the Lpar1-3 blocker Ki16425 was started after 6 months of HF–HS diet when the transaortic velocities were significantly elevated. The inhibition of Lpar1 in IGFII mice (similarly to human Lpar3 was not expressed in mouse VICs) reduced the progression rate of aortic stenosis by three-fold as evaluated with echocardiography. Consistently, the deposition of mineral in the aortic valve was decreased significantly in mice receiving Ki16425. These data thus suggest that LPAR1 could represent a novel target in order to slow the progression of CAVS. Considering that novel pharmacological compounds are in development to inhibit LPAR1, the present findings may have significant translational impact and clinical relevance.

4.4 Limitations

There are others LPARs (e.g. LPAR4-6) whose expression and role in CAVS are unknown and warrant further investigations. The mechanistic role for Lpar1 in mice could be further buttressed by the use of knockout mice. However, the *Lpar1* knockout mouse has a high perinatal mortality rate with cranial dysmorphism and intracranial haemorrhage.[38] This could be circumvented by developing conditional *Lpar1* knockout mice, which, however, would need to be crossed with genetically-modified mice that develop CAVS. Nonetheless, the present translational work contributed to highlight that a process dependent on LPAR1-p65 pS536, which is amenable to a pharmacotherapy, contributes to the progression of CAVS.

5. Conclusions

This work underscored that OxLDL-LPA promote the progression of CAVS by activating a p65 pS536 pathway downstream of LPAR1. Pharmacological inhibition of this pathway may hold promise for the development of novel therapeutic strategies to slow the progression of CAVS.

Supplementary material

Supplementary material is available at *Cardiovascular Research* online.

Acknowledgements

M.J.N., M.C.B., and P.M. conceived and designed experiments. M.J.N. and M.C.B. performed experiments in isolated lipid fractions. M.L.K. and B.J.A. isolated lipoproteins. M.J.N., M.C.B., G.M., D.A., and F.H. performed *in vitro* studies. R.B., K.L.Q., and A.D. performed echocardiography in mice. M.J.N. and M.C.B. performed analyses in mice. M.J.N. performed reporter assays and ChIP. A.M. contributed to the production of mice. P.M. drafted the manuscript. All the authors critically reviewed the manuscript and provided scientific input.

Conflict of interest: none declared.

Funding

This work was supported in part by CIHR grants to P.M. (FRN114893, FRN142244, FRN148778, FRN130254) the Heart and Stroke Foundation of Canada (G-14-0005913) and the Quebec Heart and Lung Institute Fund. B.J.A. is a research scholar from the Fonds de Recherche du Québec-Santé (FRQS). Y.B. holds a Canada Research Chair in Genomics of Heart and Lung Diseases. P.P. holds a Canada Research Chair on Heart Valve Diseases. A. Marette holds the Pfizer Research Chair on the Pathogenesis of Insulin Resistance and Cardiovascular Diseases. P.M. holds a FRQS Research Chair on the Pathobiology of Calcific Aortic Valve Disease.

References

1. Rajamannan NM, Evans FJ, Aikawa E, Grande-Allen KJ, Demer LL, Heistad DD, Simmons CA, Masters KS, Mathieu P, O'brien KD, Schoen FJ, Towler DA, Yoganathan AP, Otto CM. Calcific aortic valve disease: not simply a degenerative process: a review and agenda for research from the National Heart and Lung and Blood Institute Aortic Stenosis Working Group. Executive summary: calcific aortic valve disease-2011 update. *Circulation* 2011;**124**:1783–1791.
2. Nagy E, Eriksson P, Yousry M, Caidahl K, Ingelsson E, Hansson GK, Franco-Cereceda A, Back M. Valvular osteoclasts in calcification and aortic valve stenosis severity. *Int J Cardiol* 2013;**168**:2264–2271.
3. Mathieu P, Bouchareb R, Boulanger MC. Innate and adaptive immunity in calcific aortic valve disease. *J Immunol Res* 2015;**2015**:851945.
4. Ghosh CC, Ramaswami S, Juvekar A, Vu HY, Galdieri L, Davidson D, Vancurova I. Gene-specific repression of proinflammatory cytokines in stimulated human macrophages by nuclear IkappaBalpha. *J Immunol* 2010;**185**:3685–3693.
5. Hochrainer K, Racchumi G, Anrather J. Site-specific phosphorylation of the p65 protein subunit mediates selective gene expression by differential NF-kappaB and RNA polymerase II promoter recruitment. *J Biol Chem* 2013;**288**:285–293.
6. Sasaki CY, Barberi TJ, Ghosh P, Longo DL. Phosphorylation of RelA/p65 on serine 536 defines an I{kappa}B{alpha}-independent NF-{kappa}B pathway. *J Biol Chem* 2005;**280**:34538–34547.
7. Jang WG, Kim EJ, Kim DK, Ryoo HM, Lee KB, Kim SH, Choi HS, Koh JT. BMP2 protein regulates osteocalcin expression via Runx2-mediated Atf6 gene transcription. *J Biol Chem* 2012;**287**:905–915.
8. Smith JG, Luk K, Schulz CA, Engert JC, Do R, Hindy G, Rukh G, Dufresne L, Almgren P, Owens DS, Harris TB, Peloso GM, Kerr KF, Wong Q, Smith AV, Budoff MJ, Rotter JI, Cupples LA, Rich S, Kathiresan S, Orho-Melander M, Gudnason V, O'donnell CJ, Post WS, Thanassoulis G. Association of low-density lipoprotein cholesterol-related genetic variants with aortic valve calcium and incident aortic stenosis. *JAMA* 2014;**312**:1764–1771.
9. Thanassoulis G, Campbell CY, Owens DS, Smith JG, Smith AV, Peloso GM, Kerr KF, Pechlivanis S, Budoff MJ, Harris TB, Malhotra R, O'brien KD, Kamstrup PR, Nordestgaard BG, Tybjaerg-Hansen A, Allison MA, Aspelund T, Criqui MH, Heckbert SR, Hwang SJ, Liu Y, Sjogren M, van der Pals J, Kalsch H, Muhleisen TW, Nothen MM, Cupples LA, Caslake M, Di AE, Danesh J, Rotter JI, Sigurdsson S, Wong Q, Erbel R, Kathiresan S, Melander O, Gudnason V, O'donnell CJ, Post WS. Genetic associations with valvular calcification and aortic stenosis. *N Engl J Med* 2013;**368**:503–512.
10. Arsenault BJ, Boekholdt SM, Dube MP, Rheaume E, Wareham NJ, Khaw KT, Sandhu MS, Tardif JC. Lipoprotein(a) levels, genotype, and incident aortic valve stenosis: a prospective Mendelian randomization study and replication in a case-control cohort. *Circ Cardiovasc Genet* 2014;**7**:304–310.
11. Capoulade R, Chan KL, Yeang C, Mathieu P, Bosse Y, Dumesnil JG, Tam JW, Teo KK, Mahmut A, Yang X, Witztum JL, Arsenault BJ, Despres JP, Pibarot P, Tsimikas S. Oxidized phospholipids, lipoprotein(a) , and progression of calcific aortic valve stenosis. *J Am Coll Cardiol* 2015;**66**:1236–1246.
12. Mahmut A, Boulanger MC, El Husseini D, Fournier D, Bouchareb R, Despres JP, Pibarot P, Bosse Y, Mathieu P. Elevated expression of lipoprotein-associated phospholipase A2 in calcific aortic valve disease: implications for valve mineralization. *J Am Coll Cardiol* 2014;**63**:460–469.
13. Bouchareb R, Mahmut A, Nsaibia MJ, Boulanger MC, Dahou A, Lepine JL, Laflamme MH, Hadji F, Couture C, Trahan S, Page S, Bosse Y, Pibarot P, Scipione CA, Romagnuolo R, Koschinsky ML, Arsenault BJ, Marette A, Mathieu P. Autotaxin

derived from lipoprotein(a) and valve interstitial cells promotes inflammation and mineralization of the aortic valve. *Circulation* 2015;**132**:677–690.
14. Macphee CH, Moores KE, Boyd HF, Dhanak D, Ife RJ, Leach CA, Leake DS, Milliner KJ, Patterson RA, Suckling KE, Tew DG, Hickey DM. Lipoprotein-associated phospholipase A2, platelet-activating factor acetylhydrolase, generates two bioactive products during the oxidation of low-density lipoprotein: use of a novel inhibitor. *Biochem J* 1999;**338**(Pt 2):479–487.
15. Siess W, Zangl KJ, Essler M, Bauer M, Brandl R, Corrinth C, Bittman R, Tigyi G, Aepfelbacher M. Lysophosphatidic acid mediates the rapid activation of platelets and endothelial cells by mildly oxidized low density lipoprotein and accumulates in human atherosclerotic lesions. *Proc Natl Acad Sci U S A* 1999;**96**:6931–6936.
16. Bouchareb R, Cote N, Marie CB, Le QK, El Husseini D, Asselin J, Hadji F, Lachance D, Shayhidin EE, Mahmut A, Pibarot P, Bosse Y, Messaddeq Y, Boudreau D, Marette A, Mathieu P. Carbonic anhydrase XII in valve interstitial cells promotes the regression of calcific aortic valve stenosis. *J Mol Cell Cardiol* 2015;**82**:104–115.
17. Hadji F, Boulanger MC, Guay SP, Gaudreault N, Amellah S, Mkannez G, Bouchareb R, Marchand JT, Nsaibia MJ, Guauque-Olarte S, Pibarot P, Bouchard L, Bosse Y, Mathieu P. Altered DNA methylation of long noncoding RNA H19 in calcific aortic valve disease promotes mineralization by silencing NOTCH1. *Circulation* 2016;**134**:1848–1862.
18. Mahmut A, Boulanger MC, Bouchareb R, Hadji F, Mathieu P. Adenosine derived from ecto-nucleotidases in calcific aortic valve disease promotes mineralization through A2a adenosine receptor. *Cardiovasc Res* 2015;**106**:109–120.
19. Baker DL, Desiderio DM, Miller DD, Tolley B, Tigyi GJ. Direct quantitative analysis of lysophosphatidic acid molecular species by stable isotope dilution electrospray ionization liquid chromatography-mass spectrometry. *Anal Biochem* 2001;**292**:287–295.
20. Yung YC, Stoddard NC, Chun J. LPA receptor signaling: pharmacology, physiology, and pathophysiology. *J Lipid Res* 2014;**55**:1192–1214.
21. Cui R, Tieu B, Recinos A, Tilton RG, Brasier AR. RhoA mediates angiotensin II-induced phospho-Ser536 nuclear factor kappaB/RelA subunit exchange on the interleukin-6 promoter in VSMCs. *Circ Res* 2006;**99**:723–730.
22. Le Quang K, Bouchareb R, Lachance D, Laplante MA, El Husseini D, Boulanger MC, Fournier D, Fang XP, Avramoglu RK, Pibarot P, Deshaies Y, Sweeney G, Mathieu P, Marette A. Early development of calcific aortic valve disease and left ventricular hypertrophy in a mouse model of combined dyslipidemia and type 2 diabetes mellitus. *Arterioscler Thromb Vasc Biol* 2014;**34**:2283–2291.
23. Zhou Z, Subramanian P, Sevilmis G, Globke B, Soehnlein O, Karshovska E, Megens R, Heyll K, Chun J, Saulnier-Blache JS, Reinholz M, van ZM, Weber C, Schober A. Lipoprotein-derived lysophosphatidic acid promotes atherosclerosis by releasing CXCL1 from the endothelium. *Cell Metab* 2011;**13**:592–600.
24. Mathieu P, Boulanger MC. Basic mechanisms of calcific aortic valve disease. *Can J Cardiol* 2014;**30**:982–993.
25. Cote C, Pibarot P, Despres JP, Mohty D, Cartier A, Arsenault BJ, Couture C, Mathieu P. Association between circulating oxidised low-density lipoprotein and fibrocalcific remodelling of the aortic valve in aortic stenosis. *Heart* 2008;**94**:1175–1180.
26. O'brien KD, Reichenbach DD, Marcovina SM, Kuusisto J, Alpers CE, Otto CM. Apolipoproteins B, (a) , and E accumulate in the morphologically early lesion of 'degenerative' valvular aortic stenosis. *Arterioscler Thromb Vasc Biol* 1996;**16**:523–532.
27. Mohty D, Pibarot P, Despres JP, Cote C, Arsenault B, Cartier A, Cosnay P, Couture C, Mathieu P. Association between plasma LDL particle size, valvular accumulation of oxidized LDL, and inflammation in patients with aortic stenosis. *Arterioscler Thromb Vasc Biol* 2008;**28**:187–193.
28. Bosse Y, Miqdad A, Fournier D, Pepin A, Pibarot P, Mathieu P. Refining molecular pathways leading to calcific aortic valve stenosis by studying gene expression profile of normal and calcified stenotic human aortic valves. *Circ Cardiovasc Genet* 2009;**2**:489–498.
29. Cote N, Mahmut A, Bosse Y, Couture C, Page S, Trahan S, Boulanger MC, Fournier D, Pibarot P, Mathieu P. Inflammation is associated with the remodeling of calcific aortic valve disease. *Inflammation* 2013;**36**:573–581.
30. Moreno R, Sobotzik JM, Schultz C, Schmitz ML. Specification of the NF-kappaB transcriptional response by p65 phosphorylation and TNF-induced nuclear translocation of IKK epsilon. *Nucleic Acids Res* 2010;**38**:6029–6044.
31. Peng Y, Kim JM, Park HS, Yang A, Islam C, Lakatta EG, Lin L. AGE-RAGE signal generates a specific NF-kappaB RelA "barcode" that directs collagen I expression. *Sci Rep* 2016;**6**:18822.
32. Leon MB, Smith CR, Mack MJ, Makkar RR, Svensson LG, Kodali SK, Thourani VH, Tuzcu EM, Miller DC, Herrmann HC, Doshi D, Cohen DJ, Pichard AD, Kapadia S, Dewey T, Babaliaros V, Szeto WY, Williams MR, Kereiakes D, Zajarias A, Greason KL, Whisenant BK, Hodson RW, Moses JW, Trento A, Brown DL, Fearon WF, Pibarot P, Hahn RT, Jaber WA, Anderson WN, Alu MC, Webb JG. Transcatheter or surgical aortic-valve replacement in intermediate-risk patients. *N Engl J Med* 2016;**374**:1609–1620.
33. Mathieu P, Boulanger MC, Bouchareb R. Molecular biology of calcific aortic valve disease: towards new pharmacological therapies. *Expert Rev Cardiovasc Ther* 2014;**12**:851–862.
34. Teo KK, Corsi DJ, Tam JW, Dumesnil JG, Chan KL. Lipid lowering on progression of mild to moderate aortic stenosis: meta-analysis of the randomized placebo-controlled clinical trials on 2344 patients. *Can J Cardiol* 2011;**27**:800–808.
35. Mundy G, Garrett R, Harris S, Chan J, Chen D, Rossini G, Boyce B, Zhao M, Gutierrez G. Stimulation of bone formation in vitro and in rodents by statins. *Science* 1999;**286**:1946–1949.
36. Monzack EL, Masters KS. A time course investigation of the statin paradox among valvular interstitial cell phenotypes. *Am J Physiol Heart Circ Physiol* 2012;**303**:H903–H909.
37. Khera AV, Everett BM, Caulfield MP, Hantash FM, Wohlgemuth J, Ridker PM, Mora S. Lipoprotein(a) concentrations, rosuvastatin therapy, and residual vascular risk: an analysis from the JUPITER Trial (Justification for the Use of Statins in Prevention: an Intervention Trial Evaluating Rosuvastatin) . *Circulation* 2014;**129**:635–642.
38. Contos JJ, Fukushima N, Weiner JA, Kaushal D, Chun J. Requirement for the lpA1 lysophosphatidic acid receptor gene in normal suckling behavior. *Proc Natl Acad Sci USA* 2000;**97**:13384–13389.